Int j simul model 24 (2025) 2, 203-212
Original scientific paper

EXPERIMENTAL INVESTIGATION OF A HYDRAULIC ENGINE MOUNT BY TAGUCHI METHOD

Kamis Kocabicak, Z.
Bursa Uludag University, Faculty of Engineering, Department of Automotive Engineering, Bursa, Turkey
E-Mail: zkamis@uludag.edu.tr

Abstract
This study applied the design of experiment (DoE) to a hydraulic engine mount. Taguchi L16 orthogonal array was selected as an experimental plan, and various mounts were assembled and tested. The dynamic stiffness, K_d, values at 50 Hz frequency for ±0.1 mm vibration amplitude as the reference value were concluded. The best design combination, the priority order, and the contribution ratios of design parameters were determined by applying signal-to-noise ratio (*S/N*) and variance analysis (ANOVA). In the analyses, it was found that dynamic hardening, η, and fluid volume, V, were much more effective than other parameters on the K_d. Then, the regression analysis was applied to create two equations considering all parameters and only two effective parameters. It was obtained that K_d values calculated from the two equations were close to each other and in good agreement with the experimental results of the mounts in the DoE and the other two mounts not included in the DoE. This study has shown that analytical equations that give accurate results can be concluded for K_d via the Taguchi method.
(Received in October 2024, accepted in February 2025. This paper was with the author 2 weeks for 2 revisions.)

Key Words: Hydraulic Engine Mount, Dynamic Stiffness, Taguchi, ANOVA, Regression Analysis

1. INTRODUCTION

Engine mounts isolate vibration by holding the engine in place, thus helping to increase ride comfort. Road irregularities and engine-related vibrations affect vehicle performance negatively. Vibrations due to road irregularities have lower frequencies and high amplitudes, and engine-related vibrations occur at higher frequencies and low amplitudes. Engine mounts must dampen vibrations for both situations [1-3]. Several different types of engine mounts are available: rubber (conventional), semi-active and active mounts. Rubber mounts have insufficient damping properties at different frequencies, and semi-active and active mounts are more complex and expensive [3].

Hydraulic engine mounts provide better performance than rubber mounts for high-amplitude vibrations from the road and low-amplitude vibrations from the engine thanks to the decoupler and the inertia track. The mounts are made of rubber and metal and contain hydraulic fluid (see Fig. 1), so the damping force depends on the rubber and fluid characteristics [1, 2]. The ratio of the damping force to the vibration input is expressed as dynamic stiffness. Dynamic stiffness varies depending on the design structure and design parameters of the mount; it should be high for road irregularities and should be low for engine-related vibrations [1-4]. The effects of design parameters on the dynamic stiffness can be investigated by modeling the mount or using the design of experiment (DoE) method [4].

Various studies about hydraulic engine mounts in the literature have addressed the design, modeling, and optimization of the mounts. Design studies have generally been carried out integrated with modeling and optimization [5-7]. Modeling has been aimed at determining the dynamic behavior, and for this purpose, linear and nonlinear model approaches were discussed in the studies for hydraulic engine mounts [2, 8-11]. Various optimization methods have been applied in optimization studies, and the aim has been to improve the ride comfort of the vehicle and the dynamic properties of the mount [8, 12-16]. Since the decoupler used in hydraulic

engine mounts significantly affects the damping properties in the low and high-frequency regions, modeling and optimization studies on decouplers have also been in the literature [5, 6].

DoE applications are also a method that can be used to determine the dynamic properties of the mount. Taguchi-based DoE applications have been widely used in different fields, especially in recent years [4, 17-21], and DoE applications for hydraulic engine mounts are also available in the literature [4, 17]. Cyril and Manikandan [17] used DoE to determine the final mount location and stiffness. Kocabicak and Acar [4] applied Taguchi-based grey relational analysis for a hydraulic engine mount for high vibration amplitudes. However, no study has yet to be reported to determine mount parameters via DoE considering low vibration amplitude.

In this study, the dynamic stiffness, K_d, as the damping property of hydraulic engine mounts, was investigated experimentally according to the design parameters at low vibration amplitudes. Two levels were determined for four different design parameters, and a DoE was created using the Taguchi L16 orthogonal array approach for different design combinations. The mounts with the combinations in the DoE were tested at a vibration amplitude of ±0.1 mm in the frequency range of 0–50 Hz. Among the K_d values from the tests, K_d at 50 Hz was taken as the reference value, and signal-to-noise (*S/N*) ratio and variance analysis (ANOVA) were applied. With the analysis results, the priority orders and contribution percentages of the design parameters were calculated, and the most appropriate combination was determined. Then, by applying regression analysis, two different analytical equations were proposed for K_d according to the design parameters. In one of these equations, all parameters, and in the other, only the two parameters with high contribution were taken into account. The results obtained from both equations were close to each other and consistent with experimental results. This study shows that the equation determined by considering the contribution percentages via ANOVA could give sufficiently accurate results.

2. MATERIALS AND METHODS

2.1 Hydraulic engine mount

The most commonly used engine mounts in vehicles are hydraulic (see Fig. 1). Hydraulic engine mounts contain hydraulic fluid in addition to the metal rubber structure. Depending on the flow resistance of the fluid [18], these mounts provide different damping properties at different frequencies and vibration amplitudes. If the flow is through the decoupler, the flow resistance is low, and if it is through the inertia track because the decoupler is closed, the flow resistance is high. In this way, high damping is achieved at high vibration amplitudes at low frequencies and low damping at low vibration amplitudes at high frequencies [1-3].

Hydraulic engine mounts can be modeled according to the equivalent physical model in Fig. 2 by analyzing the continuity and momentum equations for the linear model [1, 11]. The mounts produce a damping force in response to the inputs. This force depends on the rubber characteristics and the flow within the mount. Applying Newton's second law, the transmitted force is as follows [1, 11]:

$$f = K_r x + B_r \frac{dx}{dt} + A_p P_1 \tag{1}$$

where K_r is the equivalent stiffness, B_r is the equivalent damping coefficient, P_1 is the fluid pressure, A_p is the equivalent piston area.

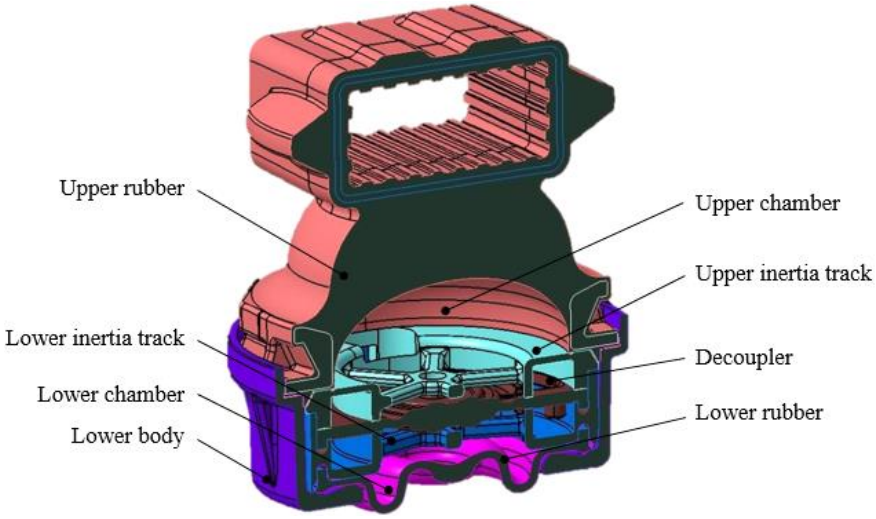


Figure 1: Hydraulic engine mount.

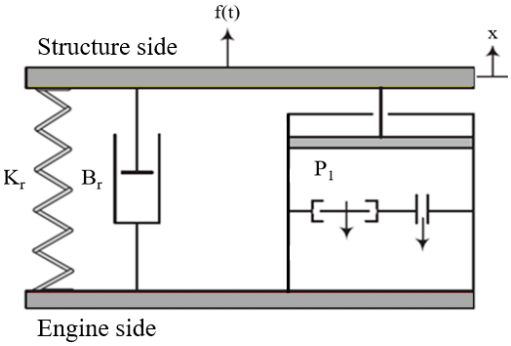


Figure 2: Equivalent physical model [1].

If a sinusoidal input ($x(t) = X \cdot sin(\omega t)$) is applied in Eq. (1), the damping force is also sinusoidal with a phase delay in the steady state ($f(t) = F \cdot sin(\omega t + \varphi)$). The force in the frequency domain is as follows ($s = j\omega$) [4, 11]:

$$F(j\omega) = K_r X(j\omega) + j\omega B_r X(j\omega) + A_p P_1(j\omega) \tag{2}$$

The frequency response transfer function, $G(j\omega)$, where input is $X(j\omega)$, and output is $F(j\omega)$, is derived as below. The dynamic stiffness of the mount, K_d, is amplitude of $G(j\omega)$, and the phase angle of the mount, φ, is the phase angle of $G(j\omega)$ [4, 11]:

$$G(j\omega) = \frac{F(j\omega)}{X(j\omega)} \tag{3}$$

$$K_d = |G(j\omega)| = \frac{F}{X} \tag{4}$$

$$\varphi = \angle G(j\omega) \tag{5}$$

K_d vary with the frequency and the damping force is proportional to K_d as seen in Eq. (4). For ride comfort at low amplitude vibrations, K_d should be lower.

2.2 Experimental setup

Hydraulic engine mounts were tested in the servohydraulic elastomer testing device in Fig. 3 (MTS 831.50). The test device has a frequency capacity of 1000 Hz, with ±10 kN force and displacements of ±20 mm [4].



Figure 3: Testing device [4].

2.3 Taguchi method

The Taguchi method is a statistical method analyzing the DoE using orthogonal arrays [17, 19-22]. It was used to find the optimum design configuration minimizing the K_d of the hydraulic engine mount at 50 Hz frequency and ±0.1 mm amplitude.

Four parameters affecting the damping behavior of hydraulic engine mounts and, therefore, K_d were determined. These are dynamic hardening, η, inertia track cross-sectional area, A, decoupler hardness, HS_d, and fluid volume, V. Dynamic hardening is the ratio of dynamic stiffness to static stiffness. Two different rubbers were used in the study, and the dynamic hardenings of these two rubbers were obtained experimentally. For the other parameters, two levels were also determined, considering the production constraints (see Table I). DoE was created in Table II according to the Taguchi L16 orthogonal array for four parameters and two levels.

In the Taguchi method, *S/N* ratios, which are the deviations of the desired values according to test results, are analyzed according to one of the performance parameters, such as smaller-the-better, larger-the-better, and nominal-the-best [4, 21]. In the study, the smaller-the-better was chosen for the K_d. The *S/N* ratio was calculated for the smaller-the-better case as below:

$$S/N = -10 log\left(\frac{1}{n}\sum_{i=1}^{n} y_i^2\right) \tag{6}$$

where y_i is the i^{th} experimental value, and n is the experiment number (n = 16).

Table I: Hydraulic engine mount design parameters and levels.

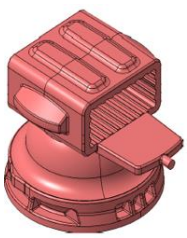
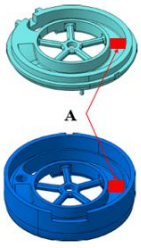
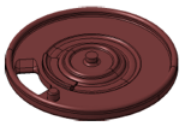
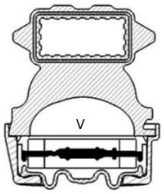
Parameters	**Dynamic hardening** η (-)	**Inertia track cross-sectional area** A (mm²)	**Decoupler hardness** HS_d (shA)	**Fluid volume** V (mm³)
				
Level 1	1.7	37.5	50	22256
Level 2	2.2	66.5	58	44512

Table II: Taguchi L16 orthogonal array.

Experiment No.	Parameters			
	η (-)	A (mm²)	HS_d (shA)	V (mm³)
1	1.7	37.5	50	22256
2	1.7	37.5	50	44512
3	1.7	37.5	58	22256
4	1.7	37.5	58	44512
5	1.7	66.5	50	22256
6	1.7	66.5	50	44512
7	1.7	66.5	58	22256
8	1.7	66.5	58	44512
9	2.2	37.5	50	22256
10	2.2	37.5	50	44512
11	2.2	37.5	58	22256
12	2.2	37.5	58	44512
13	2.2	66.5	50	22256
14	2.2	66.5	50	44512
15	2.2	66.5	58	22256
16	2.2	66.5	58	44512

3. RESULTS AND DISCUSSION

3.1 Dynamic tests

Hydraulic engine mounts, assembled according to the DoE in Table II, tested in the 1–50 Hz frequency range with an amplitude of ±0.1 mm. The preload is 750 N. The K_d variations obtained from these tests according to frequency are given in Fig. 4. As seen from the figure, K_d increases with frequency, and after approximately 10 Hz, the slope of the increase decreases and varies parallel to each other for different combinations. Since the flow at low vibration amplitudes is through the low resistance decoupler, the dynamic stiffness of the hydraulic engine mount is largely determined by the rubber properties. The mounts behave largely similarly to conventional rubber mounts [3].

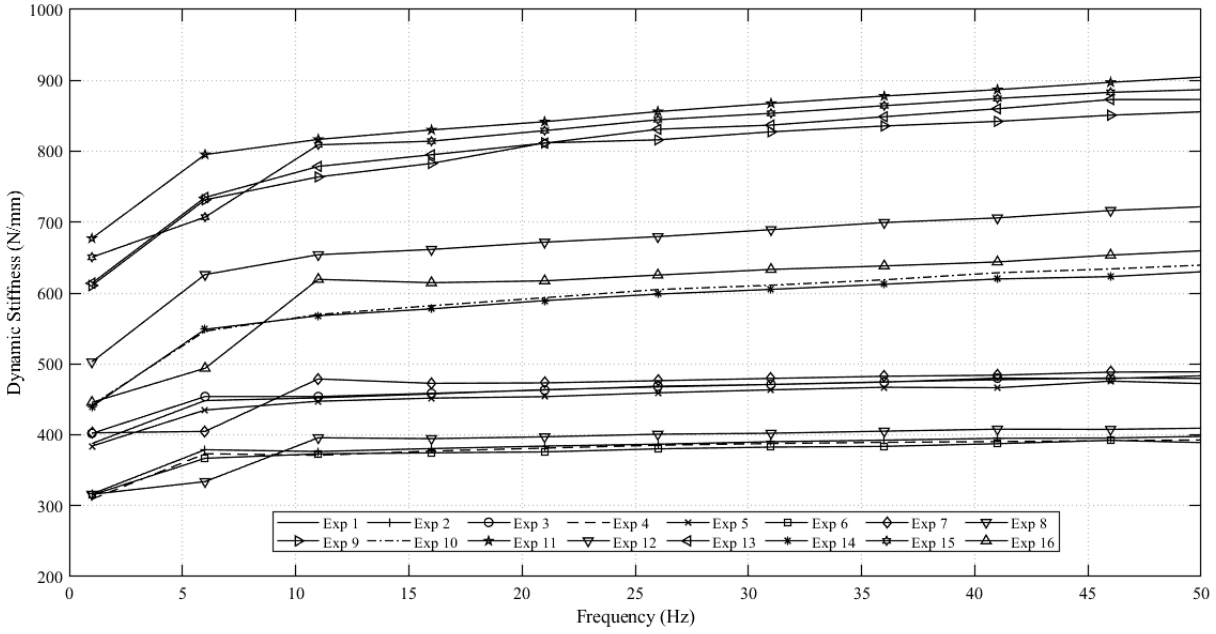


Figure 4: Dynamic stiffness variation in frequency for the ±0.1 mm vibration amplitude.

3.2 Analysis of the *S/N* ratio

K_d values at 50 Hz frequency were determined from Fig. 4 for Exp. 1–16 and these values are given in Table III. The *S/N* ratios calculated according to smaller-the-better performance characteristics for the K_d are also added in Table III. As seen from Table III, Exp. 6, which gives the largest *S/N* ratio, was determined as the most suitable design. The mean of *S/N* values according to the *S/N* analysis are given in Fig. 5 and Table IV. Considering that the level giving the largest *S/N* value is the most optimum solution [4, 17, 21], Exp. 6 was again determined as the most suitable combination. This means that $\eta = 1.7$, $A = 66.5$ mm^2, $HS_d = 50$ shA, $V = 44512$ mm^3 are the optimum configuration. The order of importance of parameters for the K_d was: $\eta > V > HS_d > A$. As seen in Fig. 5, increasing A and V increase K_d while increasing η and HS_d decrease K_d.

Table III: The experimental K_d values and *S/N* ratios.

Experiment No.	***K*$_d$ at 50 Hz** (N/mm)	***S/N*** (dB)
1	479	-53,6067
2	398	-51,9977
3	484	-53,6969
4	393	-51,8879
5	471	-53,4604
6	**388**	**-51,7766**
7	489	-53,7862
8	410	-52,2557
9	857	-58,6596
10	640	-56,1236
11	906	-59,1426
12	723	-57,1828
13	873	-58,8203
14	631	-56,0006
15	888	-58,9683
16	661	-56,4040

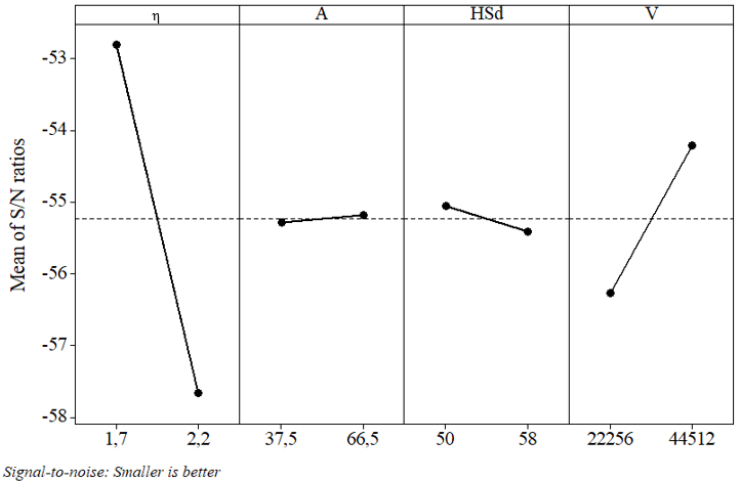


Figure 5: The effect of parameters on K_d according to mean of *S/N* ratios.

Table IV: Mean of *S/N* ratios for K_d.

Level	***η***	***A***	***HS*$_d$**	***V***
1	**-52.81**	-55.29	**-55.06**	-56.27
2	-57.66	**-55.18**	-55.42	**-54.20**
Delta	4.85	0.10	0.36	2.06
Rank	1	4	3	2

At high amplitude vibrations, the dynamic characteristics of the hydraulic engine mount depend on the phase angle, φ, as well as the dynamic stiffness, K_d. The K_d and φ curves of Exp. 6, which is determined as the most suitable combination, are given in Fig. 6 for ±1.5 mm vibration amplitude. The K_d and φ vary nonlinearly with the frequency, as seen in Fig. 6 [3, 4].

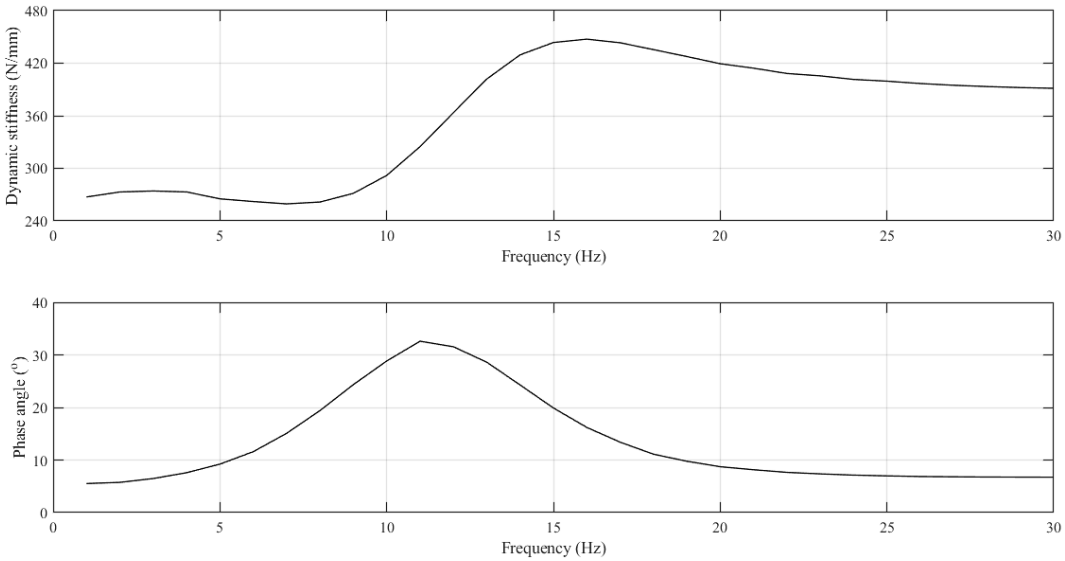


Figure 6: Dynamic characteristics in the ±1.5 mm vibration amplitude for Exp. 6.

3.3 Variance analysis (ANOVA)

The variance analysis (ANOVA) determines the percentage contribution of each parameter [4, 21, 22]. In this study, ANOVA is used to investigate which parameters significantly affect the dynamic stiffness, K_d, of the hydraulic engine mount at low amplitude vibrations. The ANOVA results are given in Table V. The *R*-Sq value was 96.15 %, so the analysis results are reliable. According to the ANOVA results in Table V, dynamic hardening, η, is the most effective parameter, with a rate of 79.41 %. The fluid volume, V, is the second effective parameter, and its contribution rate is 16.16 %. The effect rates of decoupler hardness, HS_d (0.53 %), and inertia track cross-sectional area, A (0.05 %), are quite low. Therefore, it is concluded that dynamic stiffness in low amplitude vibrations depends mainly on the rubber and the amount of fluid in the hydraulic engine mount.

Table V: ANOVA results.

Parameter	*DF*	Seq *SS*	Contribution	Adj *MS*	*F*-value	*P*-value
η	1	444556	79.41 %	444556	226.81	0.000
A	1	298	0.05 %	298	0.15	0.704
HS_d	1	2943	0.53 %	2943	1.50	0.246
V	1	90451	16.16 %	90451	46.15	0.000
Error	11	21561	3.85 %	1960		
Total	15	559807	100.00 %			

3.4 Regression analysis

In this study, regression analysis was applied to obtain the analytical equation that calculates K_d. In the first stage, the relationship between the predicted K_d values and the experimental results was modeled using a quadratic regression model (see Fig. 7). *R*-Sq was determined to be 99.5 % and *R*-Sq (adj) to be 99.4 % in the model, which shows that the model is reliable. Considering all design parameters (η, A, HS_d, V) and only two design parameters (η, V) with a

high contribution rate in ANOVA, two different analytical equations were estimated for K_d by the regression analysis. The estimated equations were determined as follows:

$$K_d = -637 + 666.7\ \eta - 0.297\ A + 3.39\ HS_d - 0.006757\ V \tag{7}$$

$$K_d = -468.9 + 666.7\ \eta - 0.006757\ V \tag{8}$$

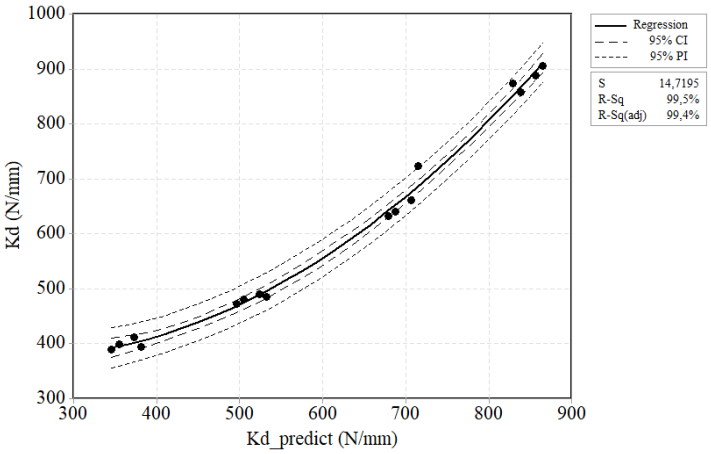


Figure 7: Quadratic regression model.

The K_d values for Exp. 1-16 in Table II were also calculated with Eqs. (7) and (8), and the results of the two equations were quite close. The calculated results were compared with the experimental results in Table III. Error percentages between the analytical and test results are given in Fig. 8. As seen in Fig. 8, the results were close to each other, and the error was a maximum of 12 %. It was concluded that regression analysis should be considered together with ANOVA; thus, estimations can be made with simpler equations.

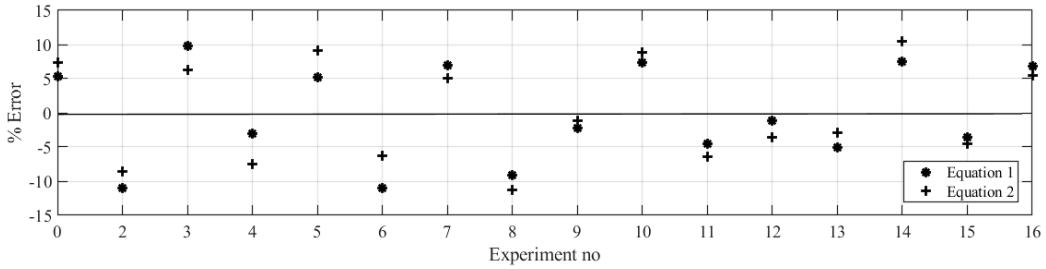


Figure 8: Error percentages between analytical and experimental results.

3.5 Experimental verification

K_d values were calculated by Eqs. (7) and (8) for another two hydraulic engine mounts with similar properties and the same outer body dimensions. These mounts were also tested in the same conditions. The analytical and experimental results are given in Table VI.

Table VI: K_d values for another hydraulic engine mounts.

Mount parameters	***K*d** (N/mm)		
	Experimental	**Eq. (7)**	**Eq. (8)**
η = 2.2, A = 79.5 mm², HS_d = 58 shA, V = 44512 mm³	633	701.98	697
η = 1.8, A = 79.5 mm², HS_d = 50 shA, V = 51223 mm³	351	362.83	385

As seen in Table VI, analytical results for both equations and test results show a rather good agreement. So, the regression model can predict the dynamic stiffness accurately. According to

these results, predictions made according to more effective parameters determined by ANOVA analysis also give accurate results.

4. CONCLUSION

In this study, the DoE method was used to determine design combinations of hydraulic engine mounts at low vibration amplitudes to consider engine vibrations. For the DoE, four parameters affecting the damping behavior of the hydraulic engine mount and two levels for these parameters were determined. DoE was created via the Taguchi L16 orthogonal array approach, and various mount configurations were assembled accordingly. All mount configurations were tested at ±0.1 mm vibration amplitude in the 0–50 Hz frequency range, and dynamic stiffnesses were measured. The dynamic stiffness, K_d, at the 50 Hz frequency was considered as the reference value for the *S/N*, variance, and regression analysis. Since the damping force of the hydraulic engine mount should be low at low amplitudes in high frequencies for driving comfort, *S/N* analysis was performed by selecting the smaller-the-better performance characteristics. According to *S/N* analysis, dynamic hardening, $\eta = 1.7$, inertia track cross-sectional area, $A = 66.5$ mm^2, decoupler hardness, $HS_d = 50$, and fluid volume, $V = 44512$ mm^3 were determined as the most suitable values, and the order of importance of the parameters was determined as $\eta > V > HS_d > A$. The contribution ratios of the parameters were determined according to ANOVA. As a result of the analysis, the contribution ratios of η and V were found to be relatively high compared to HS_d and A. Afterward, regression analysis was performed, and two analytical equations giving K_d for low amplitudes were obtained. One of the equations was obtained by considering all the parameters, and the other was obtained by considering the two parameters with high contribution rates determined in the ANOVA. The results obtained from both equations were very close to each other. Therefore, this study has shown that regression analysis can be done according to ANOVA contribution rates, and thus, results can be estimated accurately with simpler equations depending on fewer parameters. It was found that the results of both equations were in good agreement with the test results. In addition, the equations were validated with the test results of another two mounts that were not available in the DoE. Thus, it was shown that the dynamic stiffness of different mount combinations can be determined.

In summary, this study has contributed to the literature in terms of determining the parameters that are more effective in the dynamic stiffness of the hydraulic engine mounts via DoE and obtaining the analytical model according to the design parameters. In future studies, this study will extend to the mounts of different sizes and structures.

ACKNOWLEDGEMENT

The author would like to thank Bayrak Lastik Corp. for its support in the tests.

REFERENCES

[1] Marzbani, H.; Jazar, R. N.; Fard, M. (2014). Hydraulic engine mounts: a survey, *Journal of Vibration and Control*, Vol. 20, No. 10, 1439-1463, doi:10.1177/1077546312456724

[2] Shangguan, W.-B.; Lu, Z.-H. (2004). Experimental study and simulation of a hydraulic engine mount with fully coupled fluid–structure interaction finite element analysis model, *Computers & Structures*, Vol. 82, No. 22, 1751-1771, doi:10.1016/j.compstruc.2004.05.017

[3] Yu, Y.; Naganathan, N. G.; Dukkipati, R. V. (2001). A literature review of automotive vehicle engine mounting systems, *Mechanism and Machine Theory*, Vol. 36, No. 1, 123-142, doi:10.1016/S0094-114X(00)00023-9

[4] Kocabicak, Z. K.; Acar, Z. (2024). Taguchi-based grey relational analysis on multiple damping characteristics of a hydraulic engine mount, *Arabian Journal for Science and Engineering*, In Press, 12 pages, doi:10.1007/s13369-024-09510-8
[5] Christopherson, J.; Mahinfalah, M.; Jazar, R. N. (2012). Suspended decoupler: a new design of hydraulic engine mount, *Advances in Acoustics and Vibration*, Vol. 2012, No. 1, Paper 826497, 11 pages, doi:10.1155/2012/826497
[6] Fallahi, F.; Shabani, R.; Rezazadeh, G.; Tariverdilo, S. (2021). A modified design for hydraulic engine mount to improve its vibrational performance, *Proceedings of the Institution of Mechanical Engineers, Part C: Journal of Mechanical Engineering Science*, Vol. 235, No. 23, 6724-6736, doi:10.1177/09544062211000081
[7] Garmaroudi, M. A.; Mosayebi, J. (2017). Design and optimization of engine mount, *International Jornal on Energy Conversion (IRECON)*, Vol. 5, No. 4, 112-121, doi:10.15866/irecon.v5i4.13754
[8] Geisberger, A.; Khajepour, A.; Golnaraghi, F. (2002). Non-linear modelling of hydraulic mounts: theory and experiment, *Journal of Sound and Vibration*, Vol. 249, No. 2, 371-397, doi:10.1006/jsvi.2001.3860
[9] Zhang, Y.; Shangguan, W.-B.; Fang, Z. (2009). Parameter identifications of the hydraulic mount, *International Technology and Innovation Conference 2009*, 5 pages, doi:10.1049/cp.2009.1452
[10] Liu, Y.; Guan, X.; Lu, P.; Guo, R. (2021). Simulation research on dynamic characteristics of hydraulic mount, *Chinese Journal of Mechanical Engineering*, Vol. 34, Paper 49, 9 pages, doi:10.1186/s10033-021-00571-6
[11] Christopherson, J.; Jazar, G. N. (2006). Dynamic behavior comparison of passive hydraulic engine mounts. Part 1: Mathematical analysis, *Journal of Sound and Vibration*, Vol. 290, Nos. 3-5, 1040-1070, doi:10.1016/j.jsv.2005.05.008
[12] Rasekhipour, Y.; Ohadi, A. (2011). Optimization of hydraulic engine mounts through simplified and full vehicle models, *Proceedings of the World Congress on Engineering*, Vol. III, 2507-2513
[13] Ahn, Y. K.; Song, J. D.; Yang, B.-S. (2003). Optimal design of engine mount using an artificial life algorithm, *Journal of Sound and Vibration*, Vol. 261, No. 2, 309-328, doi:10.1016/S0022-460X(02)00989-6
[14] Christopherson, J.; Jazar, G. N. (2005). Optimization of classical hydraulic engine mounts based on RMS method, *Shock and Vibration*, Vol. 12, No. 2, 119-147, doi:10.1155/2005/653945
[15] Ahn, Y. K.; Song, J. D.; Yang, B.-S.; Ahn, K. K.; Morishita, S. (2005). Optimal design of nonlinear hydraulic engine mount, *Journal of Mechanical Science and Technology*, Vol. 19, No. 3, 768-777, doi:10.1007/BF02916125
[16] Hung, T. T.; Quynh, L. V.; Ha, D. V.; Huan, C. C.; Cuong, B. V.; Tan, H. A. (2021). A comparison of vehicle ride comfort performance of hydraulic engine mount system with rubber engine mount system, *ARPN Journal of Engineering and Applied Sciences*, Vol. 16, No. 23, 2610-2619
[17] Cyril, S.; Manikandan, H. (2023). Optimization of engine and transmission mounting system for a V6 front wheel drive vehicle, *Materials Today: Proceedings*, Vol. 72, No. 4, 2564-2568, doi:10.1016/j.matpr.2022.10.028
[18] Nurullayev, V.; Ismayilov, G. (2024). Graph-analytical method for determination of cavitation areas in oil pipelines in steady regime, *Proceedings on Engineering Sciences*, Vol. 6, No. 4, 1643-1652, doi:10.24874/PES06.04.023
[19] Kocabicak, Z. K.; Demir, U. (2020). Design and optimization of an electromechanical actuator for the latch of a foldable vehicle seat, *Materials Testing*, Vol. 62, No. 7, 749-755, doi:10.3139/120.111539
[20] Demir, U.; Kocabıçak, Z. K. (2021). Performance assessments of the material for the traction motor cores of an electric racing kart, *Materials Testing*, Vol. 63, No. 6, 519-528, doi:10.1515/mt-2020-0085
[21] Turan, M. K.; Topcu, E. E.; Karpat, F. (2024). Modelling and investigation of a driver seat suspension with negative stiffness structure, *International Journal of Simulation Modelling*, Vol. 23, No. 2, 275-286, doi:10.2507/IJSIMM23-2-684
[22] Singh, R. K.; Tiwari, S. K.; Srivastava, S. C.; Kumar, B. (2023). Hybrid Taguchi-GRA-CRITIC optimization method for multi-response optimization of micro-EDM drilling process parameters, *Technical Gazette*, Vol. 30, No. 3, 804-814, doi:10.17559/TV-20220601114015